

Dynamical Stability and Habitability in the HD 20794 System

STEPHEN R. KANE¹

¹*Department of Earth and Planetary Sciences, University of California, Riverside, CA 92521, USA*

ABSTRACT

The Keplerian orbit of a terrestrial planet can be a significant driver in the evolution of surface conditions, as well as influencing the overall dynamics of the system. The HD 20794 system harbors three confirmed planets orbiting a nearby G-type star, including HD 20794 d, a $\sim 5.82 M_{\oplus}$ (minimum mass) planet on a highly eccentric ($e = 0.45$) orbit that passes through the Habitable Zone (HZ). Here, we present a dynamical analysis of the HD 20794 system. We calculate the HZ boundaries and quantify the fraction of the orbital period that planet d spends within the conservative and optimistic HZ limits. Using N-body simulations, we explore the long-term orbital stability across inclinations spanning $\sim 5\text{--}90^\circ$. The system remains dynamically stable over the full 10^7 year integration for all tested inclinations, including $i = 5^\circ$ ($M_d \approx 67 M_{\oplus}$). The secular eccentricity oscillations share a common eigenperiod that scales inversely with the total system mass, consistent with Laplace-Lagrange secular theory. We examine the origin of the eccentricity of planet d, including planet-planet scattering and secular excitation from an unseen eccentric outer companion. HD 20794 d is the lowest-mass confirmed planet with $e > 0.4$ whose orbit crosses the HZ of its host star, and its periastron passage deep within the HZ makes it a likely dynamical disruptor for additional terrestrial planets, reinforcing its status as the dominant habitability prospect in the system. The proximity of HD 20794 and its inclusion on the Habitable Worlds Observatory precursor target list make this a high-priority system for understanding the interplay between orbital dynamics and planetary habitability.

Keywords: astrobiology – planetary systems – planets and satellites: dynamical evolution and stability
– stars: individual (HD 20794)

1. INTRODUCTION

The diversity of discovered planetary system architectures has provided extraordinary insight into orbital dynamics and the conditions that may permit long-term planetary habitability (Ford 2014; Winn & Fabrycky 2015; Mishra et al. 2023a,b; Horner et al. 2020; Kane et al. 2021b). A recurring challenge in evaluating the potential habitability of exoplanetary systems is the prevalence of eccentric orbits among detected planets (Shen & Turner 2008; Kane et al. 2012; Ford 2008). Planets on eccentric orbits that pass through the Habitable Zone (HZ) experience time-varying stellar flux, with potentially dramatic consequences for surface climate and atmospheric stability (Williams & Pollard 2002; Dressing et al. 2010; Kane & Gelino 2012; Armstrong et al. 2014; Kane & Torres 2017). The

dynamical architecture of a planetary system fundamentally constrains the long-term viability of orbits within the HZ (Kopparapu & Barnes 2010; Kane 2015; Kane & Blunt 2019; Kane et al. 2022). Giant planets on eccentric orbits that penetrate or approach the HZ can act as gravitational “wrecking balls”, destabilizing the orbits of terrestrial planets or precluding their formation entirely (Kane & Blunt 2019; Kane et al. 2023; Kane 2023; Kane et al. 2024; Kane 2025). Even lower-mass planets, if sufficiently eccentric, can induce secular eccentricity oscillations in neighboring bodies that drive periodic departures from temperate conditions (Hill et al. 2018, 2023; Kane & Fetherolf 2023; Kane & Burt 2024). Of particular interest are those systems where a planet of ambiguous mass resides on an eccentric orbit within the HZ, as such configurations may range from being promising candidates for habitability to dynamical disruptors, depending on the unknown orbital inclination and true planetary mass.

The HD 20794 system is an interesting case study for investigating these questions. At a distance of only 6.04 pc, HD 20794 is among the nearest G-type main-sequence stars known to host confirmed planets (Pepe et al. 2011; Nari et al. 2025). The system contains three confirmed radial velocity (RV) detected planets: HD 20794 b ($P = 18.3$ d, $M_p \sin i = 2.15 M_\oplus$), HD 20794 c ($P = 89.7$ d, $M_p \sin i = 2.98 M_\oplus$), and HD 20794 d ($P = 647.6$ d, $M_p \sin i = 5.82 M_\oplus$) (Nari et al. 2025). The inner two planets are consistent with near-circular orbits, but planet d exhibits a substantial eccentricity of $e = 0.45^{+0.10}_{-0.11}$, placing it on an orbit that traverses the stellar HZ. The planetary nature of the 647.6 d signal was initially detected by Cretignier et al. (2023) using HARPS data processed with the YARARA pipeline, and subsequently confirmed by Nari et al. (2025) using combined HARPS and ESPRESSO observations spanning more than 20 years. Despite the considerable scientific interest in this system, no comprehensive dynamical study has been conducted to date, leaving the orbital stability and habitability implications of the system unexplored.

In this paper, we present a full dynamical analysis of the HD 20794 planetary system, with a focus on the eccentric orbit of planet d and its implications for habitability. Section 2 describes the stellar and planetary properties and the calculation of the HZ boundaries. The description of the N-body simulation methodology and results of the stability analysis are presented in Section 3. In Section 4 we investigate the origin of the eccentricity of planet d. The implications for habitability and the relevance to direct imaging missions are discussed in Section 5, and we provide concluding remarks in Section 6.

2. SYSTEM ARCHITECTURE AND HABITABLE ZONE

Here we describe the HD 20794 system architecture and calculate the HZ boundaries.

2.1. Host Star

HD 20794 (82 G. Eridani, GJ 139, HIP 15510) is a bright ($V = 4.34$), nearby ($d = 6.04 \pm 0.01$ pc) G-type main-sequence star in the constellation Eridanus. We adopt the stellar parameters from the analysis of Nari et al. (2025), summarized in Table 1. The star has an effective temperature of $T_{\text{eff}} = 5368 \pm 48$ K, a luminosity of $L_\star = 0.687 \pm 0.003 L_\odot$, a mass of $M_\star = 0.79 \pm 0.01 M_\odot$, and a radius of $R_\star = 0.93 \pm 0.03 R_\odot$. A notable characteristic of HD 20794 is its subsolar metallicity ($[\text{Fe}/\text{H}] \approx -0.42$), which places it among the more metal-poor planet-hosting stars (Buchhave et al. 2014;

Table 1. Stellar parameters of HD 20794.

Parameter	Value
Spectral Type	G6V
V (mag)	4.34
Distance (pc)	6.04 ± 0.01
T_{eff} (K)	5368 ± 48
L_\star (L_\odot)	0.687 ± 0.003
M_\star (M_\odot)	0.79 ± 0.01
R_\star (R_\odot)	0.93 ± 0.03
[Fe/H]	-0.42 ± 0.02
Age (Gyr)	5.76 ± 0.66
P_{rot} (d)	~ 39

NOTE—All values adopted from Nari et al. (2025).

Brewer et al. 2018). Age estimates are uncertain, ranging from 5.76 ± 0.66 Gyr based on chromospheric activity indicators to 14^{+5}_{-6} Gyr from evolutionary track fitting (Nari et al. 2025). The low level of stellar activity, as evidenced by a magnetic cycle of ~ 3000 d and a rotation period of ~ 39 d (Nari et al. 2025), confirms the suitability of HD 20794 for high-precision RV studies. A cold debris disk has been detected at ~ 24 AU via Herschel observations (Kennedy et al. 2015), suggestive of a reservoir of icy material in the outer system. HD 20794 is included on the Habitable Worlds Observatory (HWO) Exoplanet Exploration Program precursor target list (Mamajek & Stapelfeldt 2024; Tchow et al. 2024), underscoring its importance for future direct imaging characterization efforts (Kopparapu et al. 2018; Laliotis et al. 2023; Harada et al. 2024).

2.2. Planetary Parameters

The planetary system of HD 20794 has a complex detection history that has evolved substantially over the past 15 years as RV precision and data analysis techniques have improved. Pepe et al. (2011) reported the initial discovery of three super-Earth candidates from RV observations, with orbital periods of 18.3, 40.1, and 90.3 d and minimum masses of 2.7, 2.4, and $4.8 M_\oplus$, respectively, designated planets b, c, and d. A subsequent re-analysis by Feng et al. (2017), employing a differential RV technique, found evidence for candidates at periods of 18, 89, 147, and 330 d, with weak evidence for

Table 2. Planetary parameters of the HD 20794 system.

Parameter	HD 20794 b	HD 20794 c	HD 20794 d
P (d)	18.3142 ± 0.0022	89.68 ± 0.10	$647.6^{+2.5}_{-2.7}$
K (m s^{-1})	0.614 ± 0.048	$0.502^{+0.048}_{-0.049}$	$0.567^{+0.067}_{-0.064}$
$M_p \sin i$ (M_\oplus)	2.15 ± 0.17	2.98 ± 0.29	5.82 ± 0.57
a (AU)	0.121 ± 0.001	0.350 ± 0.002	1.354 ± 0.007
e	$0.064^{+0.065}_{-0.046}$	$0.077^{+0.084}_{-0.055}$	$0.45^{+0.10}_{-0.11}$

NOTE—Values adopted from Nari et al. (2025). Semi-major axis uncertainties are estimated through error propagation.

additional signals at 43 d and 11.9 d, but did not confirm the 40.1 d planet reported by Pepe et al. (2011). Similarly, the archival RV survey of Laliotis et al. (2023) confirmed only the 18 d and 90 d planets. The non-detection of the 40.1 d signal in these later analyses, despite the increased data baseline, cast significant doubt on its planetary origin. The period of this signal is notably close to the stellar rotation period of ~ 39 d, suggesting that it may instead arise from surface activity modulation (Desort et al. 2007; Robertson et al. 2014; Nari et al. 2025).

A major advance was produced by Cretignier et al. (2023), who confirmed the 18 d and 89 d planets and detected a new candidate signal at a period of ~ 650 d. This long-period candidate was subsequently confirmed by Nari et al. (2025), who conducted a comprehensive analysis combining more than 20 years of RV observations. Nari et al. (2025) compared models with zero through four planets and found that the three-planet model (at periods of 18.3, 89.7, and 647.6 d) was strongly preferred. The additional planet candidates reported by Feng et al. (2017) at periods of 147 and 330 d were not recovered. We adopt the planetary parameters and nomenclature from Nari et al. (2025), summarized in Table 2, wherein the three confirmed planets are designated b, c, and d in order of increasing orbital period. HD 20794 d is the outermost confirmed planet and the primary focus of this investigation. The planet has a minimum mass of $M_d \sin i = 5.82 M_\oplus$, a semi-major axis of $a_d \approx 1.354$ AU, and an eccentricity of $e_d = 0.45$, yielding a periastron and apastron distances of 0.74 AU and 1.96 AU, respectively. Note that Nari et al. (2025) do not provide the periastron arguments for the planetary orbits, so we assume values of 90° for the subsequent analyses.

2.3. Habitable Zone

We calculate the HZ boundaries of HD 20794 using the formalism of Kopparapu et al. (2013, 2014). The con-

servative HZ (CHZ), defined by the runaway greenhouse and maximum greenhouse limits, spans from 0.807 AU to 1.440 AU ($S_{\text{eff}} = 1.055\text{--}0.331 F_\oplus$). The optimistic HZ (OHZ), defined by the recent Venus and early Mars empirical limits, extends from 0.637 AU to 1.519 AU ($S_{\text{eff}} = 1.693\text{--}0.298 F_\oplus$). The left panel of Figure 1 shows a top-down view of the system, including the planetary orbits overlaid on the CHZ (dark green) and OHZ (light green). The eccentric orbit of HD 20794 d carries the planet across a wide range of stellar distances during each orbital period, resulting in the planet transiting both the inner and outer boundaries of the HZ, spending only a fraction of each orbit within the temperate zone. Following the methodology described in Kane & Gelino (2012) and Kane et al. (2021a), we compute the fraction of the orbital period spent within the HZ boundaries, weighted by the time the planet spends at each orbital position. For the CHZ, HD 20794 d spends approximately 32% of its orbital period within the temperate zone, increasing to approximately 45% for the OHZ. The remaining $\sim 55\%$ of the orbit is spent exterior to the OHZ outer boundary, where the reduced stellar flux may drive surface temperatures below the freezing point of water for plausible atmospheric compositions (Kane & Gelino 2012).

The orbit-averaged incident flux provides an alternative metric for assessing the habitability of planets on eccentric orbits, particularly in terms of climate forcing (Williams & Pollard 2002; Kane et al. 2021a). The time-averaged flux is given by:

$$\langle F \rangle = \frac{L_\star}{4\pi a^2(1 - e^2)^{1/2}}, \quad (1)$$

which yields $\langle F \rangle \approx 0.42 F_\oplus$ for HD 20794 d, where F_\oplus is the flux received by Earth. Propagating the uncertainties on a and e from Table 2 yields $\langle F \rangle = 0.42^{+0.03}_{-0.02} F_\oplus$. The variation in the incident flux, relative to both the time-averaged and Earth fluxes, are depicted in the right panel of Figure 1. The time-averaged flux falls within

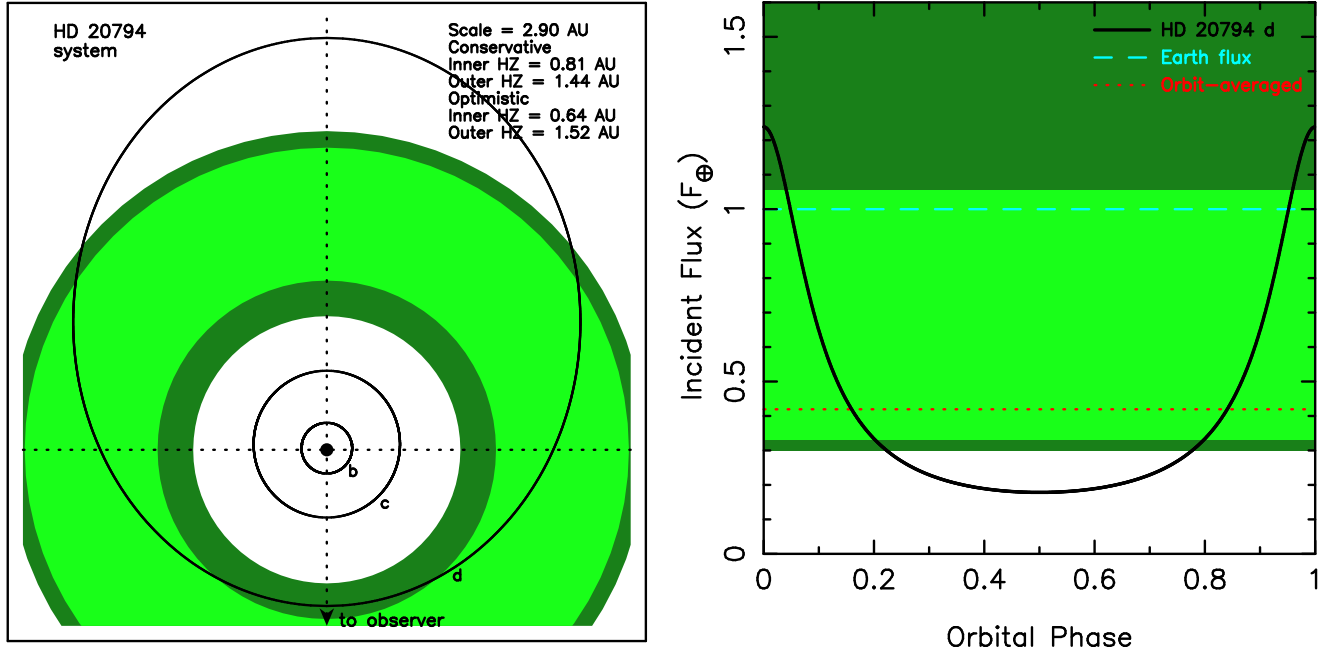


Figure 1. Left: HZ and planetary orbits in the HD 20794 system, where the orbits are labeled by planet designation. The scale of the figure is 2.9 AU along each side. Right: Variation in incident flux received by HD 20794 d during one complete orbit. For both panels, the extent of the HZ is shown in green, where light green and dark green indicate the CHZ and OHZ, respectively.

the CHZ, suggesting that on average the planet receives an insolation level consistent with temperate conditions. However, the instantaneous flux varies from $\sim 1.24 F_{\oplus}$ at periastron to $\sim 0.18 F_{\oplus}$ at apastron, a factor of ~ 7 variation that may drive extreme seasonal cycles. The periastron flux is particularly sensitive to the eccentricity uncertainty, with a 1σ range of $\sim 0.9\text{--}1.9 F_{\oplus}$, while the apastron flux is better constrained at $0.18 \pm 0.03 F_{\oplus}$.

3. DYNAMICAL ANALYSIS

Here we describe the N-body simulation methodology and present the results of the dynamical analysis.

3.1. Simulation Methodology

We conducted N-body simulations of the HD 20794 system using the Mercury Integrator Package (Chambers 1999) with a hybrid symplectic/Bulirsch-Stoer integrator and a Jacobi coordinate system (Wisdom & Holman 1991; Wisdom 2006), following the methodology described by Kane & Blunt (2019); Kane et al. (2021a, 2023). The simulations were initialized using the orbital elements from Nari et al. (2025) (Table 2), including the best-fit eccentricities. All simulations assume coplanar, prograde orbits, with the three planets sharing a common orbital inclination i with respect to the line of sight. All of the simulations were integrated for 10^7 years with a timestep of 0.1 days, orbital elements were output every 100 years,

and planetary collisions and ejections were recorded. A central goal of this study is to explore the dependence of the system stability on the true masses of the planets, which are unconstrained due to the unknown orbital inclination. We parameterize this by running suites of simulations across a grid of assumed inclinations: $i = 90^\circ, 30^\circ, 20^\circ, 10^\circ,$ and 5° . At each inclination, the true masses of all three planets are scaled as $M = M \sin i / \sin(i)$. The corresponding true masses of planet d range from $M_d \approx 5.82 M_{\oplus}$ (at $i = 90^\circ$) to $M_d \approx 66.8 M_{\oplus}$ (at $i = 5^\circ$), with the transition from the super-Earth to the Neptune-mass regime occurring at inclinations of $\sim 20^\circ$ ($M_d \sim 17 M_{\oplus}$). Empirical studies of the mass-radius relation for exoplanets have shown that the transition from predominantly rocky compositions to planets with substantial volatile envelopes occurs at $\sim 4\text{--}10 M_{\oplus}$ (Weiss & Marcy 2014; Rogers 2015; Chen & Kipping 2017; Otegi et al. 2020; Luque & Pallé 2022; Müller et al. 2024), above which planets are increasingly likely to retain thick H/He or water-rich atmospheres. The mass of Neptune ($17.15 M_{\oplus}$) provides a natural upper reference point, above which a planet would unambiguously reside in the ice giant regime. The true mass of planet d as a function of assumed inclination, along with regions of likely planetary nature, are represented in Figure 2.

3.2. Stability as a Function of Inclination

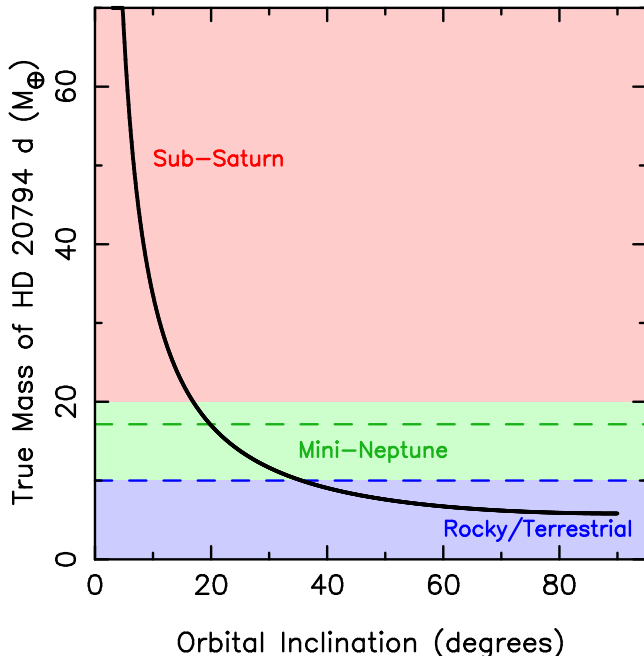


Figure 2. The true mass of planet d as a function of assumed orbital inclination. The shaded regions indicate the likely planetary nature, including terrestrial, mini-Neptune, and sub-Saturn.

The results of the inclination-dependent stability analysis demonstrate that the HD 20794 system is remarkably robust to changes in the assumed planetary masses. For all tested inclinations, from $i = 90^\circ$ ($M_d \approx 5.82 M_\oplus$) down to $i = 5^\circ$ ($M_d \approx 66.8 M_\oplus$), the three-planet system remains dynamically stable over the full 10^7 year integration, with no planetary ejections or collisions. For example, shown in Figure 3 are the simulation results for the $i = 90^\circ$ case, demonstrating the eccentricity variations and relative stability over 10^7 years for each of the three planets in the system. Additional tests at inclinations as low as $i = 1^\circ$ (corresponding to true masses exceeding $300 M_\oplus$ for planet d) also yielded stable configurations. This stability reflects the large dynamical separation between the planets: the ratio of the semi-major axes of planets c and d is $a_c/a_d \approx 0.26$, and the ratio for planets b and c is $a_b/a_c \approx 0.35$, both of which place the planets well beyond the critical spacing for orbital instability (Gladman 1993; Chambers et al. 1996; Barnes & Raymond 2004). The wide spacing, even combined with the substantial eccentricity of planet d, prevents orbit crossing for all tested mass configurations. This result demonstrates that the true mass of planet d is not constrained by the dynamical stability of the system, in contrast to many other multi-planet systems where instability provides an upper limit on the orbital inclination (Kane & Blunt 2019; Kane 2023, 2025). We note that these stability conclusions apply to the copla-

nar case; the mutual inclinations of the planets are unconstrained by RV data. However, given the wide orbital separations, modest mutual inclinations ($\lesssim 10\text{--}20^\circ$) are unlikely to alter the stability picture significantly.

3.3. Eccentricity Evolution and Secular Dynamics

Although the system remains stable at all inclinations, the secular evolution of the eccentricities reveals a rich dynamical structure that is strongly modulated by the total system mass. In all simulations, the eccentricities of the three planets undergo coupled periodic oscillations driven by the secular gravitational interaction among the planets (Murray & Dermott 1999; Laskar et al. 2004). For the minimum-mass configuration ($i = 90^\circ$), the eccentricity of planet b oscillates between ~ 0.016 and ~ 0.068 with a mean of ~ 0.045 , while planet c oscillates between ~ 0.077 and ~ 0.099 with a mean of ~ 0.088 . The eccentricity of planet d, by contrast, oscillates over a very narrow range near its initial value of 0.45, with a total amplitude of only ~ 0.0006 (see Figure 3). This behavior is characteristic of Laplace-Lagrange secular theory, where the much larger mass and eccentricity of planet d cause it to dominate the secular eigenmodes while experiencing minimal back reaction from the lower-mass inner planets (Murray & Dermott 1999; Petrovich et al. 2013).

An interesting feature of the simulations is that all three planets share a common dominant secular eigenperiod at each inclination, and this eigenperiod decreases systematically with increasing total system mass. For example, at $i = 90^\circ$ (total mass $\sim 11.0 M_\oplus$), the dominant eccentricity oscillation period is $\sim 98,000$ years. At $i = 30^\circ$ ($\sim 21.9 M_\oplus$), the period decreases to $\sim 49,000$ years, and at $i = 10^\circ$ ($\sim 63.1 M_\oplus$), the period decreases to $\sim 17,000$ years. The dominant eccentricity oscillation period for all tested inclinations down to $i = 5^\circ$ are shown in Figure 4. The product of the secular period P_{sec} and total system mass M_{total} is constant to within 0.7% across all simulations, confirming the linear scaling $P_{\text{sec}} \propto 1/M_{\text{total}}$ predicted by Laplace-Lagrange secular theory (Murray & Dermott 1999; Laskar 2008). In the Laplace-Lagrange framework, the secular eigenfrequencies are proportional to the planetary masses divided by the stellar mass and the semi-major axis ratios, so that scaling all planet masses by a common factor (as occurs when changing the system inclination) produces a proportional increase in the eigenfrequencies (Murray & Dermott 1999). The precise adherence of our simulations to this scaling confirms that the system dynamics are well described by linear secular theory over the mass range explored. Furthermore, the semi-major axes of all three planets remain effectively con-

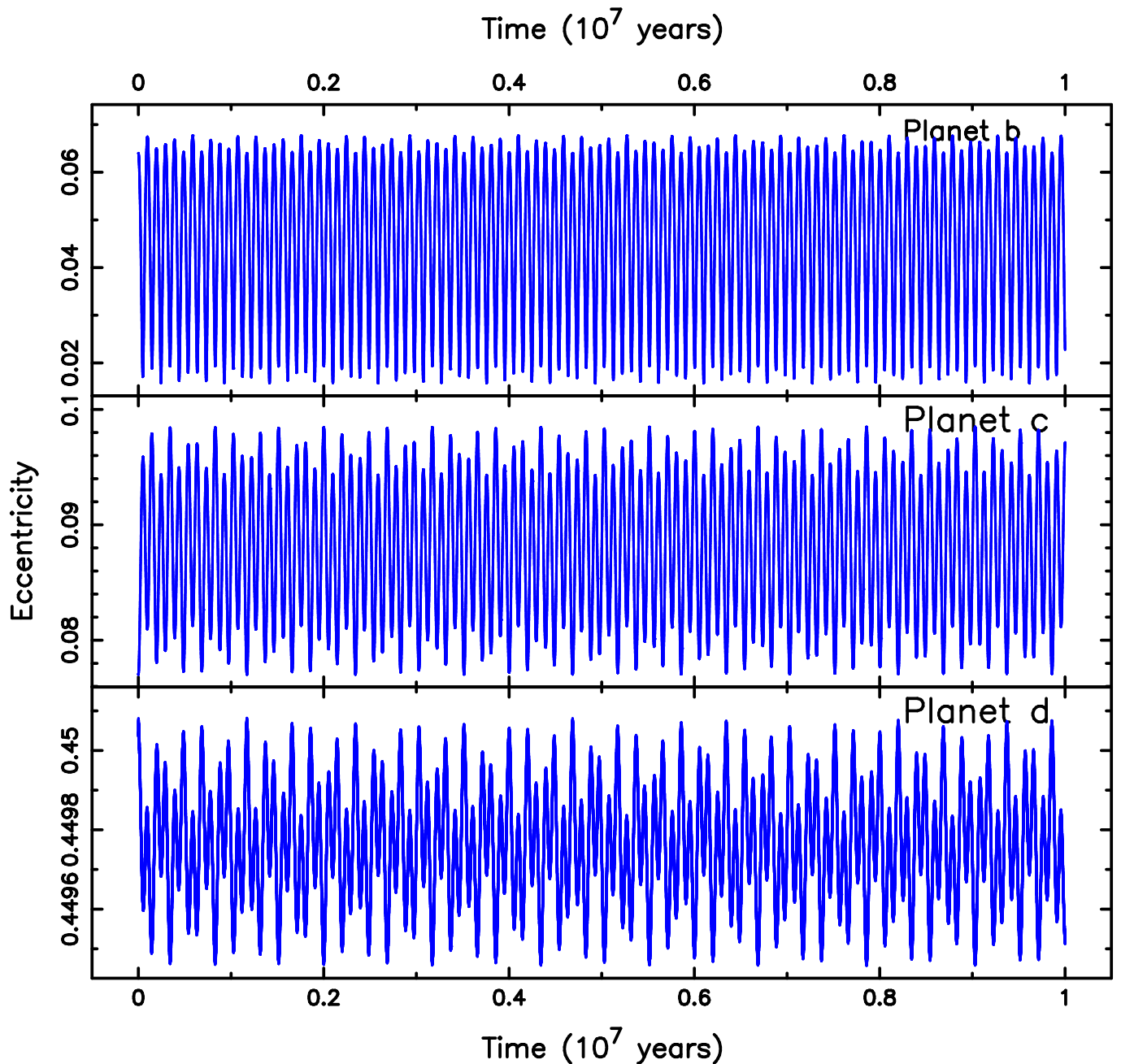


Figure 3. Eccentricity evolution for the three known planets of the HD 20794 system for the inclination case of $i = 90^\circ$. Data are shown for the full 10^7 year integration.

stant throughout the 10^7 year integrations at all tested inclinations, with variations of less than $\sim 0.01\%$. This is consistent with the conservation of semi-major axes in Laplace-Lagrange secular theory, where only the eccentricities and longitudes of periastron undergo periodic evolution (Murray & Dermott 1999). The negligible semi-major axis variability implies that the instellation variations discussed in Section 2.3 are driven entirely by the eccentricity oscillations of planet d, and do not change significantly as a function of system age.

3.4. Forced Eccentricity and Inclination Constraints

Although the dynamical stability of the system does not constrain the orbital inclination, the amplitude of the forced eccentricity oscillations of the inner planets provides an indirect observational diagnostic. The eccentricity amplitude of planet b decreases modestly from $\Delta e_b \approx 0.052$ at $i = 90^\circ$ to $\Delta e_b \approx 0.049$ at $i = 5^\circ$, and similarly for planet c ($\Delta e_c \approx 0.021$ to 0.019). These amplitudes remain consistent with the best-fit eccentricities of planets b ($e_b = 0.064^{+0.065}_{-0.046}$) and c ($e_c = 0.077^{+0.084}_{-0.055}$)

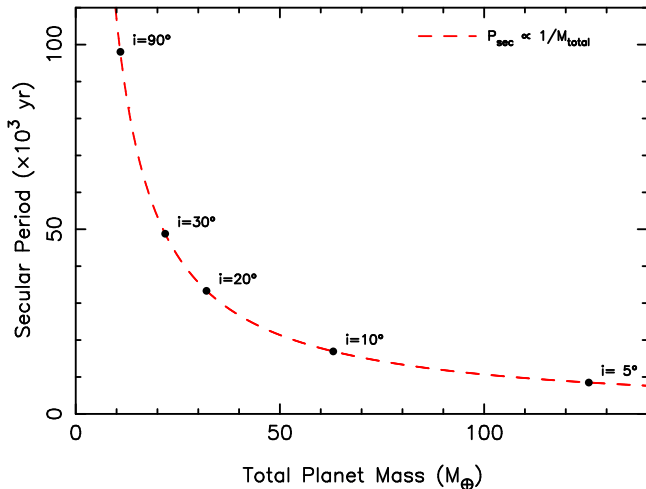


Figure 4. The dominant secular eigenperiod of the eccentricity oscillations as a function of total planet mass for the HD 20794 system. The red dashed line shows the $P_{\text{sec}} \propto 1/M_{\text{total}}$ scaling predicted by Laplace-Lagrange secular theory, which matches the simulation results to within 0.7%.

reported by Nari et al. (2025) at all tested inclinations. The near-constancy of these amplitudes across the mass range is a consequence of the secular eigenmode structure: the forced eccentricity of the inner planets is set primarily by the eccentricity of planet d and the semi-major axis ratios, with only a weak dependence on the absolute masses when all masses are scaled together (Murray & Dermott 1999). The eccentricity amplitude of planet d itself increases modestly from $\Delta e_d \approx 0.0006$ at $i = 90^\circ$ to $\Delta e_d \approx 0.0010$ at $i = 5^\circ$, reflecting the increased back reaction from the more massive inner planets.

The measured eccentricities of planets b and c are sufficiently uncertain that they do not currently constrain the system inclination. However, future observations with improved RV precision that tighten the eccentricity constraints on the inner planets could in principle probe the secular eigenmode structure and provide independent constraints on the system architecture. If the eccentricities of planets b and c are measured to be significantly below the oscillation amplitudes predicted by the simulations, this would suggest additional dissipative processes (e.g., tidal damping) or a different orbital configuration than assumed here.

4. ORIGIN OF THE ECCENTRICITY

The relatively high eccentricity of HD 20794 d is notable for a planet with a minimum mass in the super-Earth regime, as such planets are typically found on near-circular orbits (Ford 2008; Shen & Turner 2008; Kane et al. 2012; Van Eylen & Albrecht 2015). Several

mechanisms could produce or maintain this eccentricity, which we investigate here.

4.1. Planet-Planet Scattering

Planet-planet scattering is one of the most widely invoked mechanisms for producing eccentric orbits in exoplanetary systems (Rasio & Ford 1996; Chatterjee et al. 2008; Jurić & Tremaine 2008; Ford & Rasio 2008). In this scenario, gravitational interactions between two or more planets lead to close encounters that result in the ejection of one or more bodies and the excitation of the surviving planets onto eccentric orbits. If HD 20794 originally hosted an additional planet between the present orbits of planets c and d, a scattering event could have removed the interloper while pumping the eccentricity of planet d. The relatively low minimum mass of planet d makes it an atypical candidate for the scattering scenario, which more commonly involves giant planets (Chatterjee et al. 2008; Ford & Rasio 2008; Jurić & Tremaine 2008; Raymond et al. 2009a; Carrera et al. 2019). However, scattering among super-Earth-mass bodies has been demonstrated in numerical simulations (Raymond et al. 2009b), and the low metallicity of HD 20794 may have favored the formation of multiple super-Earths rather than a single giant planet.

A useful diagnostic for assessing the degree of dynamical excitation is the angular momentum deficit (AMD), which quantifies the difference between the angular momentum of the actual system and that of the equivalent circular, coplanar configuration (Laskar 1997; Laskar & Petit 2017; Murray & Dermott 1999). For the minimum-mass, coplanar configuration of HD 20794 based on the parameters in Table 2, the circular angular momenta of the three planets are $\Lambda_b = 1.77 \times 10^{40}$, $\Lambda_c = 4.17 \times 10^{40}$, and $\Lambda_d = 1.60 \times 10^{41} \text{ kg m}^2 \text{ s}^{-1}$, yielding a total circular angular momentum of $\Lambda_{\text{tot}} = 2.20 \times 10^{41} \text{ kg m}^2 \text{ s}^{-1}$. For comparison, the angular momentum values for Venus and Earth are 1.84×10^{40} and $2.66 \times 10^{40} \text{ kg m}^2 \text{ s}^{-1}$, respectively. The corresponding HD 20794 system AMD is $1.73 \times 10^{40} \text{ kg m}^2 \text{ s}^{-1}$, or $\approx 7.9\%$ of the total circular angular momentum budget. The AMD is overwhelmingly dominated by planet d, which contributes $\approx 99.1\%$ of the total AMD. Because these calculations adopt the RV minimum masses, both Λ_k and the AMD scale approximately as $1/\sin i$ for a common coplanar inclination, while the fractional dominance of planet d remains essentially unchanged. Figure 5 shows the mass and semi-major axis of an additional planet (on a circular orbit) that alone would produce the system AMD. Many of these configurations are likely unviable due to a destabilization of the system, but a subset may provide the seed for a scattering

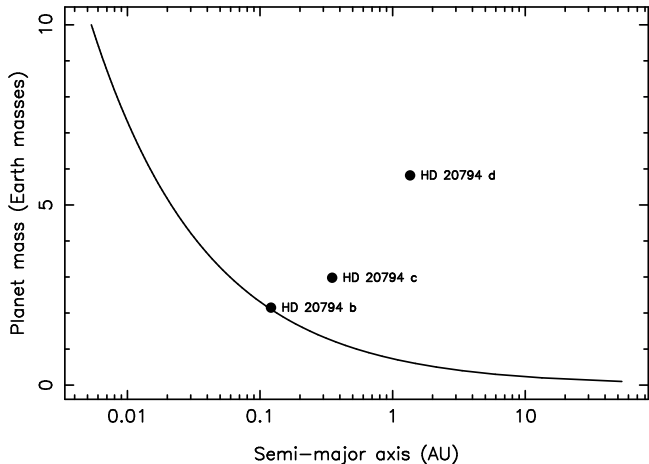


Figure 5. The mass and semi-major axis of an additional planet in a circular orbit whose angular momentum equals the angular momentum deficit (AMD) for the HD 20794 system, and may have been previously ejected from the system. The dots indicate the minimum masses and semi-major axes of the known planets in the system.

event that resulted in the present system architecture (Kane et al. 2023).

The concentration of the system AMD in the outer planet is consistent with a history in which the present architecture was dynamically excited after formation, whether by scattering or by another secular process, although the AMD alone does not uniquely identify the excitation origin (Laskar & Petit 2017). Meanwhile, the wide spacing of the planets implies that the system remains AMD-stable in the sense of Laskar & Petit (2017) and Petit et al. (2017). Despite the substantial AMD stored in planet d, there is insufficient angular momentum exchange available to drive orbit crossing between adjacent planets. This is consistent with the long-term N-body integrations described in Section 3, which show stability for all tested inclinations.

4.2. Secular Excitation from an Outer Companion

An unseen outer companion on a moderately eccentric orbit could excite the eccentricity of planet d through secular perturbations (Kane & Raymond 2014; Petrovich 2015; Anderson & Lai 2017). Nari et al. (2025) reported sensitivity to companions with true masses of $\sim 50 M_{\oplus}$ at orbital distances of 3–10 AU, and found no evidence for additional Keplerian signals with periods exceeding 2000 d or a long-term acceleration trend. This effectively rules out Neptune-mass or larger companions within ~ 10 AU on favorably inclined orbits. However, a giant planet at larger separations (10–20 AU) could still be present below the current detection threshold, particularly if it resides on a low-inclination orbit that minimizes the RV signal.

An additional configuration that is particularly difficult to exclude is one in which the outer companion itself resides on a highly eccentric orbit. The detectability of a Keplerian signal in RV data depends sensitively on the orbital eccentricity, with the induced stellar reflex motion becoming increasingly concentrated near the brief periastron passage as e increases (Cumming 2004; Kane 2007, 2013). For sufficiently high eccentricities, the bulk of the orbit is spent near apastron where the RV amplitude is substantially reduced, such that a companion may evade detection unless the observational baseline captures a periastron passage. This mechanism is particularly attractive in the context of HD 20794 d for two reasons. First, it naturally reconciles the absence of a long-term RV trend with the existence of a sufficiently massive outer perturber, as the time-averaged reflex motion of the host star would be small compared to the peak amplitude near periastron. Second, a highly eccentric outer companion is a natural source of AMD, which would be exchanged with planet d through secular coupling and could account for the observed eccentricity without requiring a scattering event in the system’s dynamical history (Nagasawa et al. 2008; Naoz et al. 2013). A companion with $e \gtrsim 0.5$ at semi-major axes of 10–30 AU would be consistent with the current RV non-detection while also providing the secular forcing necessary to maintain the eccentricity of planet d over gigayear timescales.

The Herschel-detected debris disk at ~ 24 AU (Kennedy et al. 2015) may provide indirect evidence for such a companion, as debris disk structure is often shaped by the gravitational influence of nearby planets (Wyatt et al. 2012). Future observations with longer temporal baselines and astrometric constraints from Gaia will be essential for testing this hypothesis (Perryman et al. 2014; Holl et al. 2023).

5. DISCUSSION

5.1. Habitability Implications

The dynamical analysis presented here reveals a complex picture for the habitability of the HD 20794 system. The system is dynamically stable at all tested inclinations, meaning that planet d retains its orbit regardless of its true mass, and the inner planets are not disrupted even in the most extreme mass scenarios. This stability ensures that the HZ of the system is dynamically accessible, a key prerequisite for habitability (Kane et al. 2024; Kane & Burt 2024).

If planet d is indeed a $\sim 6 M_{\oplus}$ rocky world (i.e., the system is viewed near edge-on), then its eccentric orbit carries it through the HZ with a time-averaged flux consistent with temperate conditions. However, the large

eccentricity produces extreme seasonal variations in incident flux, with a factor of ~ 7 difference between periastron and apastron. Climate modeling of Earth-like planets on eccentric orbits suggests that atmospheres with sufficient thermal inertia (e.g., those with substantial CO_2 inventories or deep oceans) can buffer the extreme flux variations and maintain above-freezing temperatures for a significant fraction of the orbit, even for eccentricities as large as 0.4–0.5 (Williams & Pollard 2002; Dressing et al. 2010; Way & Georgakarakos 2017). The orbit-averaged flux of $\langle F \rangle \approx 0.42 F_\oplus$ for HD 20794 d is well within the range explored by such studies, suggesting that habitable conditions are at least plausible.

Three-dimensional general circulation model (GCM) simulations provide the most detailed predictions for the climate response to eccentric orbits (Shields et al. 2016; Way & Georgakarakos 2017; Wolf et al. 2017; Way et al. 2023; Leconte et al. 2013). For an Earth analog with $e = 0.4$, Way & Georgakarakos (2017) found that the ocean thermal inertia is sufficient to prevent complete surface freezing during apastron passage, though significant ice-sheet advance and retreat occurs on orbital timescales. The 647.6 d orbital period of HD 20794 d is long enough that such “flash-freezing” cycles would be driven primarily by the atmospheric response time rather than the ocean’s deeper thermal reservoir. The relatively low orbit-averaged flux ($\sim 0.42 F_\oplus$) places HD 20794 d near the outer edge of the conservative HZ, where the climate sensitivity to CO_2 partial pressure becomes a critical factor (Kopparapu et al. 2013; Shields et al. 2016). A dedicated GCM study of HD 20794 d, incorporating the measured orbital parameters and a range of atmospheric compositions, would be a valuable follow-up to the dynamical analysis presented here.

If the true mass of planet d is significantly higher than the minimum mass, for example $\sim 10\text{--}20 M_\oplus$ corresponding to inclinations of $\sim 17\text{--}34^\circ$, then the planet would more likely be a mini-Neptune with a thick volatile envelope (Rogers 2015; Otegi et al. 2020; Müller et al. 2024), rendering it inhospitable to Earth-based life. Moreover, at such masses the eccentric orbit of planet d would exert a strong dynamical influence on any terrestrial planet residing elsewhere within the HZ. Previous dynamical studies have shown that even a mildly eccentric sub-Neptune in or near the HZ can destabilize the orbits of additional temperate planets in the same system, substantially reducing the phase space within which habitable worlds may reside (Kane & Fetherolf 2023; Kane & Burt 2024). In the case of HD 20794, the periastron of planet d (0.74 AU) lies deep within the HZ, such that gravitational per-

turbations from planet d would be strongly felt by any additional HZ bodies. The combination of an eccentric orbit, a potentially substantial mass, and a periastron passage within the HZ therefore makes planet d a potential dynamical disruptor for any other HZ planet in the system, regardless of whether planet d itself is rocky or volatile-rich. This reinforces the importance of the current three-planet architecture: if planet d is habitable, it is likely the sole habitable world in the HD 20794 system, with the notable exception of subsurface ocean environments analogous to those hypothesized for the Jovian and Saturnian satellites (Lunine 2017).

5.2. Relevance to HWO and Future Direct Imaging

HD 20794 is included on the HWO ExEP precursor science stars list (Mamajek & Stapelfeldt 2024), and the proximity of the system ($d = 6.04$ pc) makes it exceptionally favorable for direct imaging characterization at visible and near-infrared wavelengths (Nari et al. 2025). Shown in Figure 6 are the predicted projected and angular separations of HD 20794 d from the host star over one complete orbit. The two panels of Figure 6 represent the extreme inclination scenarios of $i = 90^\circ$ (left) and $i = 0^\circ$ (right), the latter of which corresponds to a face-on orbit. The angular separation of planet d from the host star depends on the inclination, ranging from $\sim 0.0\text{--}0.20''$ for the $i = 90^\circ$ case and $\sim 0.12\text{--}0.33''$ for the $i = 0^\circ$ case, placing it within the accessible regime of a 6-meter class space telescope with a coronagraph (Harada et al. 2024). Additionally, Laliotis et al. (2023) provided RV sensitivity constraints for HD 20794 in the context of future direct imaging missions, further underscoring the importance of a comprehensive dynamical characterization. Systems in which the known planets are stable and the HZ is dynamically accessible are preferred targets for atmospheric characterization (Kane et al. 2024; Kane & Burt 2024). The dynamical stability demonstrated here at all tested inclinations strengthens the case for HD 20794 as a high-priority target, with planet d itself representing the most promising HZ candidate in the system given the likely dynamical constraints on additional HZ bodies (Section 5.1).

The HD 20794 system is also a compelling target for the Large Interferometer for Exoplanets (LIFE) mission concept (Quanz et al. 2022a), which would characterize terrestrial exoplanet atmospheres in the mid-infrared through space-based nulling interferometry. The mid-infrared offers complementary atmospheric diagnostics to those accessible at visible wavelengths, including thermal emission features of CO_2 , O_3 , and H_2O that are critical biosignature and habitability indicators (Schwieterman et al. 2018; Quanz et al.

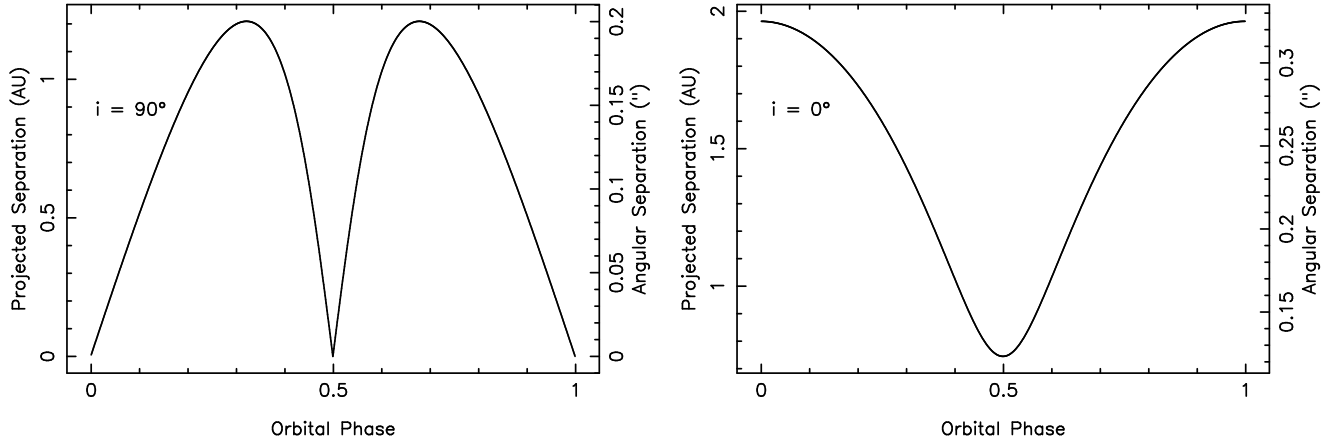


Figure 6. Projected and angular separation of HD 20794 d from the host star, assuming inclinations of $i = 90^\circ$ (left) and $i = 0^\circ$ (right). An orbital phase of zero corresponds to the location of superior conjunction.

2022b; Fujii et al. 2018). The combination of HWO reflected-light and LIFE thermal-emission observations would provide a comprehensive atmospheric characterization of planet d (Fujii et al. 2018; Catling et al. 2018; Alei et al. 2024), enabling robust constraints on its surface temperature, atmospheric composition, and potential habitability across the full range of its eccentric orbit.

5.3. Comparison to Other Eccentric HZ Planets

The majority of known planets on eccentric orbits that traverse the HZ are giant planets with masses of order $\sim M_J$. These include HR 5183 b (Blunt et al. 2019; Kane et al. 2019), the recently characterized companions in the Gaia-4 and Gaia-5 systems (Stefánsson et al. 2025; Kane 2025), and numerous other cases cataloged through RV surveys (Kane et al. 2012; Kane & Gelino 2012; Kane et al. 2021a). For such massive planets, habitability of the planet itself is not plausible, but the orbital dynamics have implications for any terrestrial bodies that may share the HZ. HD 20794 d occupies a fundamentally different regime. At $M_p \sin i = 5.82 M_\oplus$ with $e = 0.45$, it is the lowest (minimum) mass confirmed planet with an eccentricity exceeding 0.4 whose orbit crosses the HZ of its host star. This combination of low mass and high eccentricity is exceedingly rare among the known exoplanet population: statistical studies of the eccentricity distribution consistently find that super-Earths and sub-Neptunes ($M_p \lesssim 20 M_\oplus$) reside on near-circular orbits, with mean eccentricities of $\langle e \rangle \approx 0.04$ – 0.06 for compact multi-planet systems (Shen & Turner 2008; Kane et al. 2012). Fewer than five confirmed planets below $20 M_\oplus$ have eccentricities exceeding 0.4.

The closest comparator in the literature is Gl 514 b, a super-Earth with $M_p \sin i \approx 5.2 M_\oplus$ on a sim-

ilarly eccentric orbit ($e \approx 0.45$) that crosses the HZ of its M-dwarf host at 7.6 pc (Damasso et al. 2022). Biasiotti et al. (2024) conducted a comprehensive climate study of Gl 514 b using the EOS-ESTM seasonal-latitudinal energy balance model, demonstrating that habitability remains achievable for plausible atmospheric compositions despite the large flux variations, but is sensitive to CO_2 abundance, rotation period, and ocean fraction. A comparable climate investigation of HD 20794 d, incorporating the measured orbital parameters and a range of atmospheric and surface configurations, would represent a natural extension of the Gl 514 b study to the G-dwarf regime. Despite the similarities in mass and eccentricity between Gl 514 b and HD 20794 d, the two planets occupy quite different stellar environments: Gl 514 b orbits an M dwarf, where the XUV environment, tidal effects, and spectral energy distribution differ substantially from the G-dwarf host of HD 20794. HD 20794 d is therefore the only confirmed super-Earth on a highly eccentric HZ-crossing orbit around a Sun-like star within 10 pc.

The rarity of this parameter combination underscores its scientific value. The high eccentricity of planet d cannot be easily explained by the dynamical interactions among the three known planets alone (Section 4.1), and the low mass makes conventional planet-planet scattering an unlikely formation pathway. The proximity of the host star ($d = 6.04$ pc), its inclusion on the HWO precursor target list (Mamajek & Stapelfeldt 2024; Tuchow et al. 2024; Harada et al. 2024), and the availability of a Sun-like stellar spectrum for atmospheric retrieval modeling make HD 20794 d an important test case for understanding whether habitable conditions can persist on planets with large orbital eccentricities around solar-type stars.

6. CONCLUSIONS

The HD 20794 system provides a compelling laboratory for studying the relationship between orbital dynamics and planetary habitability. The CHZ spans 0.807–1.440 AU, and HD 20794 d spends approximately 32% of its orbital period within this zone, with an orbit-averaged flux of $\langle F \rangle \approx 0.42 F_{\oplus}$ consistent with temperate conditions for an Earth-like atmosphere. N-body simulations reveal that the three-planet system is dynamically stable at all tested inclinations, from $i = 90^{\circ}$ ($M_d \approx 5.8 M_{\oplus}$) down to $i = 5^{\circ}$ ($M_d \approx 66.8 M_{\oplus}$), over the full 10^7 year integration. The eccentricities of all three planets undergo coupled secular oscillations whose eigenperiod scales inversely with the total system mass, in precise agreement with Laplace-Lagrange secular theory. The eccentricity of planet d remains tightly confined near its initial value of $e \approx 0.45$, while the inner planets exhibit forced eccentricity amplitudes ($\Delta e_b \approx 0.05$, $\Delta e_c \approx 0.02$) that are consistent with the measured eccentricities at all inclinations. The true planetary masses are therefore not constrained by the dynamical stability of the system, but may be probed by future high-precision eccentricity measurements of the inner planets. The origin of the eccentricity of planet d remains uncertain, with planet-planet scattering, secular excitation from an unseen outer companion, and primordial eccentricity all viable mechanisms that require further observational constraints.

The proximity of HD 20794 ($d = 6.04$ pc) and its inclusion on the HWO precursor target list make this

system a high-priority case for understanding the dynamical prerequisites for habitability in multi-planet systems. The dynamical stability demonstrated here at all inclinations strengthens the case for HD 20794 as a viable direct imaging target, and the system is also compelling for the LIFE mid-infrared interferometry concept. We note, however, that the eccentric orbit of planet d carries its periastron deep into the HZ, such that planet d is likely to act as a dynamical disruptor for any additional terrestrial planets within the HZ (Kane & Fetherolf 2023; Kane & Burt 2024). Planet d therefore represents the dominant HZ target in the system, and its habitability is not contingent on a companion population of temperate worlds. Future work should incorporate three-dimensional GCM simulations to quantify the surface temperature evolution of HD 20794 d over its eccentric orbit, and further investigation of the debris disk at ~ 24 AU may illuminate the dynamical history of the outer system and the prospects for volatile delivery to the inner planets.

ACKNOWLEDGEMENTS

The author would like to thank the anonymous reviewer for their useful feedback on the manuscript. This research has made use of the Habitable Zone Gallery at hzglory.org. The results reported herein benefited from collaborations and/or information exchange within NASA’s Nexus for Exoplanet System Science (NExSS) research coordination network sponsored by NASA’s Science Mission Directorate.

Software: Mercury (Chambers 1999)

REFERENCES

- Alei, E., Quanz, S. P., Konrad, B. S., et al. 2024, A&A, 689, A245, doi: [10.1051/0004-6361/202450320](https://doi.org/10.1051/0004-6361/202450320)
- Anderson, K. R., & Lai, D. 2017, MNRAS, 472, 3692, doi: [10.1093/mnras/stx2250](https://doi.org/10.1093/mnras/stx2250)
- Armstrong, D. J., Gómez Maqueo Chew, Y., Faedi, F., & Pollacco, D. 2014, MNRAS, 437, 3473, doi: [10.1093/mnras/stt2146](https://doi.org/10.1093/mnras/stt2146)
- Barnes, R., & Raymond, S. N. 2004, ApJ, 617, 569, doi: [10.1086/423419](https://doi.org/10.1086/423419)
- Biasiotti, L., Simonetti, P., Vladilo, G., et al. 2024, MNRAS, 530, 4300, doi: [10.1093/mnras/stae1124](https://doi.org/10.1093/mnras/stae1124)
- Blunt, S., Endl, M., Weiss, L. M., et al. 2019, AJ, 158, 181, doi: [10.3847/1538-3881/ab3e63](https://doi.org/10.3847/1538-3881/ab3e63)
- Brewer, J. M., Wang, S., Fischer, D. A., & Foreman-Mackey, D. 2018, ApJL, 867, L3, doi: [10.3847/2041-8213/aae710](https://doi.org/10.3847/2041-8213/aae710)
- Buchhave, L. A., Bizzarro, M., Latham, D. W., et al. 2014, Nature, 509, 593, doi: [10.1038/nature13254](https://doi.org/10.1038/nature13254)
- Carrera, D., Raymond, S. N., & Davies, M. B. 2019, A&A, 629, L7, doi: [10.1051/0004-6361/201935744](https://doi.org/10.1051/0004-6361/201935744)
- Catling, D. C., Krissansen-Totton, J., Kiang, N. Y., et al. 2018, Astrobiology, 18, 709, doi: [10.1089/ast.2017.1737](https://doi.org/10.1089/ast.2017.1737)
- Chambers, J. E. 1999, MNRAS, 304, 793, doi: [10.1046/j.1365-8711.1999.02379.x](https://doi.org/10.1046/j.1365-8711.1999.02379.x)
- Chambers, J. E., Wetherill, G. W., & Boss, A. P. 1996, Icarus, 119, 261, doi: [10.1006/icar.1996.0019](https://doi.org/10.1006/icar.1996.0019)
- Chatterjee, S., Ford, E. B., Matsumura, S., & Rasio, F. A. 2008, ApJ, 686, 580, doi: [10.1086/590227](https://doi.org/10.1086/590227)
- Chen, J., & Kipping, D. 2017, ApJ, 834, 17, doi: [10.3847/1538-4357/834/1/17](https://doi.org/10.3847/1538-4357/834/1/17)
- Cretignier, M., Dumusque, X., Aigrain, S., & Pepe, F. 2023, A&A, 678, A2, doi: [10.1051/0004-6361/202347232](https://doi.org/10.1051/0004-6361/202347232)

- Cumming, A. 2004, *MNRAS*, 354, 1165, doi: [10.1111/j.1365-2966.2004.08275.x](https://doi.org/10.1111/j.1365-2966.2004.08275.x)
- Damasso, M., Perger, M., Almenara, J. M., et al. 2022, *A&A*, 666, A187, doi: [10.1051/0004-6361/202243522](https://doi.org/10.1051/0004-6361/202243522)
- Desort, M., Lagrange, A. M., Galland, F., Udry, S., & Mayor, M. 2007, *A&A*, 473, 983, doi: [10.1051/0004-6361:20078144](https://doi.org/10.1051/0004-6361:20078144)
- Dressing, C. D., Spiegel, D. S., Scharf, C. A., Menou, K., & Raymond, S. N. 2010, *ApJ*, 721, 1295, doi: [10.1088/0004-637X/721/2/1295](https://doi.org/10.1088/0004-637X/721/2/1295)
- Feng, F., Tuomi, M., & Jones, H. R. A. 2017, *A&A*, 605, A103, doi: [10.1051/0004-6361/201730406](https://doi.org/10.1051/0004-6361/201730406)
- Ford, E. B. 2008, *AJ*, 135, 1008, doi: [10.1088/0004-6256/135/3/1008](https://doi.org/10.1088/0004-6256/135/3/1008)
- . 2014, *Proceedings of the National Academy of Science*, 111, 12616, doi: [10.1073/pnas.1304219111](https://doi.org/10.1073/pnas.1304219111)
- Ford, E. B., & Rasio, F. A. 2008, *ApJ*, 686, 621, doi: [10.1086/590926](https://doi.org/10.1086/590926)
- Fujii, Y., Angerhausen, D., Deitrick, R., et al. 2018, *Astrobiology*, 18, 739, doi: [10.1089/ast.2017.1733](https://doi.org/10.1089/ast.2017.1733)
- Gladman, B. 1993, *Icarus*, 106, 247, doi: [10.1006/icar.1993.1169](https://doi.org/10.1006/icar.1993.1169)
- Harada, C. K., Dressing, C. D., Kane, S. R., & Ardestani, B. A. 2024, *ApJS*, 272, 30, doi: [10.3847/1538-4365/ad3e81](https://doi.org/10.3847/1538-4365/ad3e81)
- Hill, M. L., Bott, K., Dalba, P. A., et al. 2023, *AJ*, 165, 34, doi: [10.3847/1538-3881/aca1c0](https://doi.org/10.3847/1538-3881/aca1c0)
- Hill, M. L., Kane, S. R., Seperuelo Duarte, E., et al. 2018, *ApJ*, 860, 67, doi: [10.3847/1538-4357/aac384](https://doi.org/10.3847/1538-4357/aac384)
- Holl, B., Sozzetti, A., Sahlmann, J., et al. 2023, *A&A*, 674, A10, doi: [10.1051/0004-6361/202244161](https://doi.org/10.1051/0004-6361/202244161)
- Horner, J., Kane, S. R., Marshall, J. P., et al. 2020, *PASP*, 132, 102001, doi: [10.1088/1538-3873/ab8eb9](https://doi.org/10.1088/1538-3873/ab8eb9)
- Jurić, M., & Tremaine, S. 2008, *ApJ*, 686, 603, doi: [10.1086/590047](https://doi.org/10.1086/590047)
- Kane, S. R. 2007, *MNRAS*, 380, 1488, doi: [10.1111/j.1365-2966.2007.12144.x](https://doi.org/10.1111/j.1365-2966.2007.12144.x)
- . 2013, *ApJ*, 766, 10, doi: [10.1088/0004-637X/766/1/10](https://doi.org/10.1088/0004-637X/766/1/10)
- . 2015, *ApJL*, 814, L9, doi: [10.1088/2041-8205/814/1/L9](https://doi.org/10.1088/2041-8205/814/1/L9)
- . 2023, *AJ*, 166, 187, doi: [10.3847/1538-3881/acfb01](https://doi.org/10.3847/1538-3881/acfb01)
- . 2025, *AJ*, 170, 329, doi: [10.3847/1538-3881/ae17c9](https://doi.org/10.3847/1538-3881/ae17c9)
- Kane, S. R., & Blunt, S. 2019, *AJ*, 158, 209, doi: [10.3847/1538-3881/ab4c3e](https://doi.org/10.3847/1538-3881/ab4c3e)
- Kane, S. R., & Burt, J. A. 2024, *AJ*, 168, 279, doi: [10.3847/1538-3881/ad8a68](https://doi.org/10.3847/1538-3881/ad8a68)
- Kane, S. R., Ciardi, D. R., Gelino, D. M., & von Braun, K. 2012, *MNRAS*, 425, 757, doi: [10.1111/j.1365-2966.2012.21627.x](https://doi.org/10.1111/j.1365-2966.2012.21627.x)
- Kane, S. R., & Fetherolf, T. 2023, *AJ*, 166, 205, doi: [10.3847/1538-3881/acff5a](https://doi.org/10.3847/1538-3881/acff5a)
- Kane, S. R., & Gelino, D. M. 2012, *Astrobiology*, 12, 940, doi: [10.1089/ast.2011.0798](https://doi.org/10.1089/ast.2011.0798)
- Kane, S. R., Li, Z., Turnbull, M. C., Dressing, C. D., & Harada, C. K. 2024, *AJ*, 168, 195, doi: [10.3847/1538-3881/ad6a50](https://doi.org/10.3847/1538-3881/ad6a50)
- Kane, S. R., Li, Z., Wolf, E. T., Ostberg, C., & Hill, M. L. 2021a, *AJ*, 161, 31, doi: [10.3847/1538-3881/abcbfd](https://doi.org/10.3847/1538-3881/abcbfd)
- Kane, S. R., & Raymond, S. N. 2014, *ApJ*, 784, 104, doi: [10.1088/0004-637X/784/2/104](https://doi.org/10.1088/0004-637X/784/2/104)
- Kane, S. R., & Torres, S. M. 2017, *AJ*, 154, 204, doi: [10.3847/1538-3881/aa8f8e](https://doi.org/10.3847/1538-3881/aa8f8e)
- Kane, S. R., Dalba, P. A., Li, Z., et al. 2019, *AJ*, 157, 252, doi: [10.3847/1538-3881/ab1ddf](https://doi.org/10.3847/1538-3881/ab1ddf)
- Kane, S. R., Arney, G. N., Byrne, P. K., et al. 2021b, *Journal of Geophysical Research (Planets)*, 126, e06643, doi: [10.1002/jgre.v126.2](https://doi.org/10.1002/jgre.v126.2)
- Kane, S. R., Foley, B. J., Hill, M. L., et al. 2022, *AJ*, 163, 20, doi: [10.3847/1538-3881/ac366b](https://doi.org/10.3847/1538-3881/ac366b)
- Kane, S. R., Hill, M. L., Dalba, P. A., et al. 2023, *AJ*, 165, 252, doi: [10.3847/1538-3881/acd17a](https://doi.org/10.3847/1538-3881/acd17a)
- Kennedy, G. M., Matrà, L., Marmier, M., et al. 2015, *MNRAS*, 449, 3121, doi: [10.1093/mnras/stv511](https://doi.org/10.1093/mnras/stv511)
- Kopparapu, R. K., & Barnes, R. 2010, *ApJ*, 716, 1336, doi: [10.1088/0004-637X/716/2/1336](https://doi.org/10.1088/0004-637X/716/2/1336)
- Kopparapu, R. K., Ramirez, R. M., SchottelKotte, J., et al. 2014, *ApJ*, 787, L29, doi: [10.1088/2041-8205/787/2/L29](https://doi.org/10.1088/2041-8205/787/2/L29)
- Kopparapu, R. K., Ramirez, R., Kasting, J. F., et al. 2013, *ApJ*, 765, 131, doi: [10.1088/0004-637X/765/2/131](https://doi.org/10.1088/0004-637X/765/2/131)
- Kopparapu, R. K., Hébrard, E., Belikov, R., et al. 2018, *ApJ*, 856, 122, doi: [10.3847/1538-4357/aab205](https://doi.org/10.3847/1538-4357/aab205)
- Lalot, K., Burt, J. A., Mamajek, E. E., et al. 2023, *AJ*, 165, 176, doi: [10.3847/1538-3881/acc067](https://doi.org/10.3847/1538-3881/acc067)
- Laskar, J. 1997, *A&A*, 317, L75
- . 2008, *Icarus*, 196, 1, doi: [10.1016/j.icarus.2008.02.017](https://doi.org/10.1016/j.icarus.2008.02.017)
- Laskar, J., & Petit, A. C. 2017, *A&A*, 605, A72, doi: [10.1051/0004-6361/201630022](https://doi.org/10.1051/0004-6361/201630022)
- Laskar, J., Robutel, P., Joutel, F., et al. 2004, *A&A*, 428, 261, doi: [10.1051/0004-6361:20041335](https://doi.org/10.1051/0004-6361:20041335)
- Leconte, J., Forget, F., Charnay, B., Wordsworth, R., & Pottier, A. 2013, *Nature*, 504, 268, doi: [10.1038/nature12827](https://doi.org/10.1038/nature12827)
- Lunine, J. I. 2017, *Acta Astronautica*, 131, 123, doi: [10.1016/j.actaastro.2016.11.017](https://doi.org/10.1016/j.actaastro.2016.11.017)
- Luque, R., & Pallé, E. 2022, *Science*, 377, 1211, doi: [10.1126/science.abl7164](https://doi.org/10.1126/science.abl7164)
- Mamajek, E., & Stapelfeldt, K. 2024, arXiv e-prints, arXiv:2402.12414, doi: [10.48550/arXiv.2402.12414](https://doi.org/10.48550/arXiv.2402.12414)
- Mishra, L., Alibert, Y., Udry, S., & Mordasini, C. 2023a, *A&A*, 670, A68, doi: [10.1051/0004-6361/202243751](https://doi.org/10.1051/0004-6361/202243751)

- . 2023b, *A&A*, 670, A69,
doi: [10.1051/0004-6361/202244705](https://doi.org/10.1051/0004-6361/202244705)
- Müller, S., Baron, J., Helled, R., Bouchy, F., & Parc, L. 2024, *A&A*, 686, A296,
doi: [10.1051/0004-6361/202348690](https://doi.org/10.1051/0004-6361/202348690)
- Murray, C. D., & Dermott, S. F. 1999, *Solar System Dynamics* (Cambridge University Press),
doi: [10.1017/CBO9781139174817](https://doi.org/10.1017/CBO9781139174817)
- Nagasawa, M., Ida, S., & Bessho, T. 2008, *ApJ*, 678, 498,
doi: [10.1086/529369](https://doi.org/10.1086/529369)
- Naoz, S., Farr, W. M., Lithwick, Y., Rasio, F. A., & Teyssandier, J. 2013, *MNRAS*, 431, 2155,
doi: [10.1093/mnras/stt302](https://doi.org/10.1093/mnras/stt302)
- Nari, N., Dumusque, X., Hara, N. C., et al. 2025, *A&A*, 693, A297, doi: [10.1051/0004-6361/202451769](https://doi.org/10.1051/0004-6361/202451769)
- Otegi, J. F., Bouchy, F., & Helled, R. 2020, *A&A*, 634, A43, doi: [10.1051/0004-6361/201936482](https://doi.org/10.1051/0004-6361/201936482)
- Pepe, F., Lovis, C., Ségransan, D., et al. 2011, *A&A*, 534, A58, doi: [10.1051/0004-6361/201117055](https://doi.org/10.1051/0004-6361/201117055)
- Perryman, M., Hartman, J., Bakos, G. Á., & Lindegren, L. 2014, *ApJ*, 797, 14, doi: [10.1088/0004-637X/797/1/14](https://doi.org/10.1088/0004-637X/797/1/14)
- Petit, A. C., Laskar, J., & Boué, G. 2017, *A&A*, 607, A35,
doi: [10.1051/0004-6361/201731196](https://doi.org/10.1051/0004-6361/201731196)
- Petrovich, C. 2015, *ApJ*, 805, 75,
doi: [10.1088/0004-637X/805/1/75](https://doi.org/10.1088/0004-637X/805/1/75)
- Petrovich, C., Malhotra, R., & Tremaine, S. 2013, *ApJ*, 770, 24, doi: [10.1088/0004-637X/770/1/24](https://doi.org/10.1088/0004-637X/770/1/24)
- Quanz, S. P., Ottiger, M., Fontanet, E., et al. 2022a, *A&A*, 664, A21, doi: [10.1051/0004-6361/202140366](https://doi.org/10.1051/0004-6361/202140366)
- Quanz, S. P., Absil, O., Benz, W., et al. 2022b, *Experimental Astronomy*, 54, 1197,
doi: [10.1007/s10686-021-09791-z](https://doi.org/10.1007/s10686-021-09791-z)
- Rasio, F. A., & Ford, E. B. 1996, *Science*, 274, 954,
doi: [10.1126/science.274.5289.954](https://doi.org/10.1126/science.274.5289.954)
- Raymond, S. N., Armitage, P. J., & Gorelick, N. 2009a, *ApJL*, 699, L88, doi: [10.1088/0004-637X/699/2/L88](https://doi.org/10.1088/0004-637X/699/2/L88)
- Raymond, S. N., O'Brien, D. P., Morbidelli, A., & Kaib, N. A. 2009b, *Icarus*, 203, 644,
doi: [10.1016/j.icarus.2009.05.016](https://doi.org/10.1016/j.icarus.2009.05.016)
- Robertson, P., Mahadevan, S., Endl, M., & Roy, A. 2014, *Science*, 345, 440, doi: [10.1126/science.1253253](https://doi.org/10.1126/science.1253253)
- Rogers, L. A. 2015, *ApJ*, 801, 41,
doi: [10.1088/0004-637X/801/1/41](https://doi.org/10.1088/0004-637X/801/1/41)
- Schwieterman, E. W., Kiang, N. Y., Parenteau, M. N., et al. 2018, *Astrobiology*, 18, 663, doi: [10.1089/ast.2017.1729](https://doi.org/10.1089/ast.2017.1729)
- Shen, Y., & Turner, E. L. 2008, *ApJ*, 685, 553,
doi: [10.1086/590548](https://doi.org/10.1086/590548)
- Shields, A. L., Barnes, R., Agol, E., et al. 2016, *Astrobiology*, 16, 443, doi: [10.1089/ast.2015.1353](https://doi.org/10.1089/ast.2015.1353)
- Stefánsson, G., Mahadevan, S., Winn, J. N., et al. 2025, *AJ*, 169, 107, doi: [10.3847/1538-3881/ada9e1](https://doi.org/10.3847/1538-3881/ada9e1)
- Tuchow, N. W., Stark, C. C., & Mamajek, E. 2024, *AJ*, 167, 139, doi: [10.3847/1538-3881/ad25ec](https://doi.org/10.3847/1538-3881/ad25ec)
- Van Eylen, V., & Albrecht, S. 2015, *ApJ*, 808, 126,
doi: [10.1088/0004-637X/808/2/126](https://doi.org/10.1088/0004-637X/808/2/126)
- Way, M. J., & Georgakarakos, N. 2017, *ApJ*, 835, L1,
doi: [10.3847/2041-8213/835/1/L1](https://doi.org/10.3847/2041-8213/835/1/L1)
- Way, M. J., Ostberg, C., Foley, B. J., et al. 2023, *SSRv*, 219, 13, doi: [10.1007/s11214-023-00953-3](https://doi.org/10.1007/s11214-023-00953-3)
- Weiss, L. M., & Marcy, G. W. 2014, *ApJL*, 783, L6,
doi: [10.1088/2041-8205/783/1/L6](https://doi.org/10.1088/2041-8205/783/1/L6)
- Williams, D. M., & Pollard, D. 2002, *International Journal of Astrobiology*, 1, 61, doi: [10.1017/S1473550402001064](https://doi.org/10.1017/S1473550402001064)
- Winn, J. N., & Fabrycky, D. C. 2015, *ARA&A*, 53, 409,
doi: [10.1146/annurev-astro-082214-122246](https://doi.org/10.1146/annurev-astro-082214-122246)
- Wisdom, J. 2006, *AJ*, 131, 2294, doi: [10.1086/500829](https://doi.org/10.1086/500829)
- Wisdom, J., & Holman, M. 1991, *AJ*, 102, 1528,
doi: [10.1086/115978](https://doi.org/10.1086/115978)
- Wolf, E. T., Shields, A. L., Kopparapu, R. K., Haqq-Misra, J., & Toon, O. B. 2017, *ApJ*, 837, 107,
doi: [10.3847/1538-4357/aa5ffc](https://doi.org/10.3847/1538-4357/aa5ffc)
- Wyatt, M. C., Kennedy, G., Sibthorpe, B., et al. 2012, *MNRAS*, 424, 1206,
doi: [10.1111/j.1365-2966.2012.21298.x](https://doi.org/10.1111/j.1365-2966.2012.21298.x)